

## Body segments angle computation from single view

Tomislav Pribanić, Peter Sturm, Ivan Brigić

► **To cite this version:**

Tomislav Pribanić, Peter Sturm, Ivan Brigić. Body segments angle computation from single view. International Symposium on the 3-D Analysis of Human Movement, 2006, Valenciennes, France. 2006. <inria-00384322>

**HAL Id: inria-00384322**

**<https://hal.inria.fr/inria-00384322>**

Submitted on 14 May 2009

**HAL** is a multi-disciplinary open access archive for the deposit and dissemination of scientific research documents, whether they are published or not. The documents may come from teaching and research institutions in France or abroad, or from public or private research centers.

L'archive ouverte pluridisciplinaire **HAL**, est destinée au dépôt et à la diffusion de documents scientifiques de niveau recherche, publiés ou non, émanant des établissements d'enseignement et de recherche français ou étrangers, des laboratoires publics ou privés.

# Body segments angle computation from single view

Tomislav Pribanic\*, Peter Sturm\*\*, Ivan Brigic\*\*\*

Faculty of electrical engineering and computing, University of Zagreb, Zagreb, Croatia\*

INRIA Rhône-Alpes, Montbonnot St Martin, France\*\*

Faculty of Kinesiology, University of Zagreb, Zagreb, Croatia\*\*\*

tomislav.pribanic@fer.hr, peter.sturm@inria.fr, ivan.brigic@zg.htnet.hr

**Abstract**—During the human motion analysis it would be beneficial if it were accurate method for computing angles between segments using single camera and possibly even noncalibrated one. Main goal of this work was to test one possible such implementation based on rather familiar concept involving vanishing points and the image of the absolute conic. Proposed method evaluated with synthetic data is still inferior to ‘classical’ ways of angle computation. Still, its attractive practical advantages warrant further investigation which should ultimately yield improvement in accuracy.

**Keywords**- *human motion analysis; camera calibration; absolute conic; vanishing point; segments angle;*

## I. INTRODUCTION

Biomechanical analysis of human motion very often encompasses 2D or 3D reconstruction. There are number of approaches for 3D reconstruction, including use of electromagnetic sensors, acoustic sensors, accelerometers, photogrammetric principles [1] etc. Every method has (dis)advantages and the particular method of choice is usually dictated by the specific characteristic of the final application. Perhaps one of the major advantages of photogrammetric methods is a fact of method being practically 100% noninvasive, since it is based on processing images acquired by cameras ([2], [3]). In general for full 3D spatial reconstruction minimum of two cameras (views) are needed, unless certain assumptions are included ([4], [5]). On the other hand 2D reconstruction is doable with single camera, but with rather strong condition that subject's movement has to remain in a plane, i.e. two dimensional [6]. In either case prerequisite for spatial reconstruction is camera calibration step [7].

The particular method of calibration is a major issue when it comes down to convince of the end user. In that sense calibration is expected to be easy and fast, satisfying at the same time desired degree of the ultimate 3D reconstruction accuracy. Calibration methods have evolved in the last few decades from those using traditional and rather cumbersome 3D calibration cages to more user friendly methods based on 2D calibration planes or even using solely wand of known length ([8], [9], [10]). From algebraic point of view calibration is a procedure during which parameters describing mapping from space into image plane are computed. Usually computed camera's parameters are divided in external ones and internal

ones. Former group is describing what is known as camera position and orientation in space, and later group features camera's internal characteristics [11].

Typical output of 3D reconstruction systems are spatial positions of certain number of points, usually markers attached to human body surface. Furthermore velocity and acceleration can be then trivially calculated. These are kinematic data and not surprisingly such reconstruction systems are frequently referred as 3D kinematic systems. In addition, number of other biomechanical parameters can be computed too, such as: angles, angular velocities, angular accelerations [12]. Not to mention that some 3D kinematic systems provide also so called body segment parameters (BSP, typically segment's masses, center of masses, principal moment of inertia ...). BSP combined with kinematic data into Newton-Euler equations of motion provide kinetic parameters of human motion (inverse dynamic principle [13], [14]). Biomechanical analyses can be even more comprehensive including force platform data, EMG signals, ECG signals and so forth. Nevertheless many researches have based, at least one part, of their conclusions considering single parameter only, such as angle between body segments ([1], [6]).

As implicated above, to compute angle between two segments in space one needs generally to perform 3D reconstruction of certain number of points on segments. The precondition to do that is of course camera calibration along with all potential problems concerning it, regardless of the concrete calibration method applied. Therefore, it appears to be beneficial to avoid unnecessary steps such as full camera calibration and/or reconstruction in cases where one is interested for instance only in segments angle. Moreover, it would be practical if we would need only one camera to do that. This paper presents an idea to compute spatial angle between segments using single camera, i.e. view. The proposed idea completely discards necessity for calibration of external parameters and internal parameters as well; reasonably assuming that for good quality cameras internals can be read from camera's data sheet. The idea is based on practical implementation of rather known concept in projective geometry: absolute conic. Thus, the next subsection will first briefly describe geometric entity called absolute conic.

## II. PROPOSED METHOD

### A. Absolute conic

The complete description and properties of the absolute conic and its image can be found elsewhere ([11], [15]). Here, only the basics will be reviewed. The absolute conic is a conic on the plane at infinity, consisting of points  $\mathbf{X}$  such that

$$\begin{aligned} X &= [x \ y \ z \ t] \quad t = 0 \\ x^2 + y^2 + z^2 &= 0 \end{aligned} \quad (1)$$

where points with  $t=0$  are called points at infinity and their images are so called vanishing points  $\mathbf{v}$ . Writing the first three components of point  $\mathbf{X}$  separately as  $\mathbf{d}$  the defining equation for the absolute conic within the plane at infinity, has even simpler form:

$$\begin{aligned} d &= [x \ y \ z]^T \\ d^T \cdot d &= 0 \end{aligned} \quad (2)$$

Let us recall the decomposition of a camera's projection matrix  $\mathbf{P}$  [3]:

$$\begin{aligned} P &= K \cdot [R | -R \cdot t] \\ K &= \begin{bmatrix} f_x & 0 & u_0 \\ 0 & f_y & v_0 \\ 0 & 0 & 1 \end{bmatrix} \quad t = \begin{bmatrix} tx \\ ty \\ tz \end{bmatrix} \end{aligned} \quad (3)$$

where  $\mathbf{K}$  is the upper triangular matrix of internal camera parameters ( $f_x$  and  $f_y$  focal lengths;  $u_0$ ,  $v_0$  principal point),  $\mathbf{R}$  and  $\mathbf{t}$  represent external camera parameters (orientation and position). The image point (i.e. vanishing point) corresponding to a point at infinity mapped by a camera with matrix  $\mathbf{P}$  (3) is given by

$$v = P \cdot [d \ 0]^T = K \cdot R \cdot d \quad (4)$$

Solving (4) for  $\mathbf{d}$  and combining with (2) gives:

$$v^T \cdot (K \cdot K^T)^{-1} \cdot v = v^T \cdot \omega \cdot v \quad (5)$$

Image point  $\mathbf{v}$  is on the image of the absolute conic if and only if (5) is equal to zero. Thus, the image of the absolute conic is a plane conic  $\omega$  represented by the matrix  $(\mathbf{K}\mathbf{K}^T)^{-1}$ . It can further be shown that the angle  $\alpha$  between two lines in 3D space can be found using the information about the vanishing points  $\mathbf{v}_1$  and  $\mathbf{v}_2$  of those two lines and  $\omega$ :

$$\cos \alpha = \frac{v_1^T \cdot \omega \cdot v_2}{\sqrt{(v_1^T \cdot \omega \cdot v_1) \cdot (v_2^T \cdot \omega \cdot v_2)}} \quad (6)$$

Conversely, if the angle between two lines is known we have a constraint on  $\omega$ . Generally, the above equation is quadratic. However, assuring that the angle between the lines is  $90^\circ$  will give us a linear constraint:

$$v_1^T \cdot \omega \cdot v_2 = 0 \quad (7)$$

Obviously, the internal camera parameters are neatly embedded in the IAC and once the matrix  $\omega$  is found, its Cholesky

decomposition would yield us the matrix  $\mathbf{K}$  itself. For completeness, alternatives in practice to find  $\mathbf{K}$  from  $\omega$  can be found in [16].

### B. Vanishing points determination

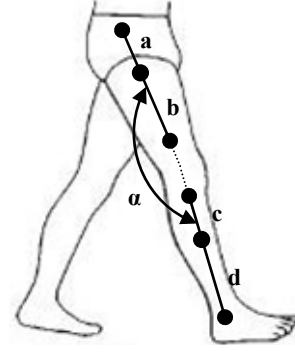


Figure 1. Potential setup of wands attachment with markers for  $\alpha$  angle computation with known distances  $a$ ,  $b$ ,  $c$  and  $d$

Let us assume that we are able to identify lines representing two segments (i.e. segments longitudinal axes). According to the above equation (6) if we know vanishing points of two lines and given the internal parameters of the camera in context, then we are able to compute angle between those two lines, i.e. body segments in our case. How to compute vanishing points? Putting different set of markers on human segments is rather common way of computing various kinematic and kinetic parameters. Apart from apparent disadvantages, primarily in terms of time needed to attach number of markers, there are numerous advantages specifically in terms of computational effort and accuracy compare to the case when markerless approach would have been used for the same matter. Consequently many biomechanics go even one step further in their research where they attach on human body segments different sticks, plates etc. which should further simplify computation and strengthen the accuracy. Therefore in the spirit of the similar reasoning it is believed during the course of this work that attaching similar structure on the segments is reasonable compromise. More specifically, Fig. 1 shows potential alternative to calculate angle for lower extremities. It should be clear from the general structure of proposed attachment on Fig. 1 that attached wands are lines representing, i.e. being parallel to, longitudinal axis of the upper leg and lower leg. Furthermore on each wand there are three markers preferably coated with material sensitive to IR light and thus relatively easily detectable with accompanying IR cameras.

Knowing two distances (i.e. identifying three markers) on a certain wand is sufficient to find position of vanishing point on the camera's image plane. In brief, the act of the camera imaging can be understood as projection from 1D projective space (wand in 3D Euclidean space) to another 1D projective space (wand's image in camera's image plane). Homography responsible for that projection is described by homogenous  $2 \times 2$   $\mathbf{H}$  matrix which elements can be calculated from minimum of three pairs of point correspondences between

mentioned 1D projective spaces. Once  $\mathbf{H}$  is obtained it is trivial to find image of the point at infinity, i.e. vanishing point in the cameras image plane.

This concludes the basic theory behind proposed idea. In summary, attaching two wands on segments, in manner similar to one shown on Fig. 1, we are able to find spatial angle between segments using only two pieces of information: wands direction (segments longitudinal axes) vanishing points and camera's internal parameters. First piece of information is relatively easily achievable by identification of three wand markers on the image. And cameras internals are either taken from data sheets, if possible, or from some earlier calibration. No need for full calibration and/or use of multiple cameras, solving correspondences problems between them etc.

### III. METHOD EVALUATION

Proposed idea was evaluated using noise free synthetic data and then adding Gauss noise with zero mean and different amounts of variance on image coordinates. In more detail, one typical cameras setup for biomechanical analyses of human motion was used. There were nine cameras stationed around imaginary calibration volume of size  $3\text{m} \times 3\text{m} \times 2\text{m}$ . Taken cameras parameters for all nine cameras are given in Table I. Two wands each having three markers on ( $a=15\text{cm}$ ,  $b=20\text{cm}$ ,  $c=10\text{cm}$ ,  $d=15\text{cm}$ ) and enclosing random angle were randomly translated on different locations within calibration volume. In particular there were 5000 different locations within calibration volume where two wands formed each time different angle. Hence, there were 5000 various angles to be computed. Angles formed by two wands were computed in two different ways. First one assumed proposed idea where vanishing points of wands, on each spatial location, were computed and used along the camera internal matrix to compute angle (6). It was done for all nine cameras. Second approach assumed 'classical' way of computing spatial angle first, where 3D reconstructions of wands markers were preformed, based on both external and internal parameters in Table I. Therefore the angle between those two lines was found simply as angle between direction vectors of the reconstructed lines, i.e. markers on it. Furthermore, 3D reconstructions were preformed one time using all 9 cameras and later also using various camera pairs.

Table II shows mean error, in degrees, between true angles and computed one when using proposed method. First column of the table concerns the camera in context. The next columns show the mean error for particular amount of added Gauss noise (expressed as variance) and some camera. For example, second column shows mean error when variance of added noise to ideal image coordinates was set to zero (i.e. computing with noise free data, mean error was zero), second column resembles situation when added noise variance was increased to 0.01 etc. Table III shows similar result as in Table II, but when 'classical' approach was undertaken. First row of results (i.e. CamAll) concerns when all 9 available cameras were used for 3D reconstruction of wand markers. And calculation of angles were based on such data (as explained above), again under the different amounts of added amount of noise. The next rows are concerned when only different camera pairs were used for 3D reconstruction; just as it were the only two possible

cameras to work with. For instance second row (Cam12) includes results for camera 1 and camera 2 forming a pair. In total there are 36 possible pair combinations for 9 cameras. Due to limited space in Table III are shown only 6 representative pairs.

TABLE I. CAMERAS PARAMETERS

| Cam. Num. | Internal Parameters |     |                      |     | External parameters           |         |          |                        |     |      |
|-----------|---------------------|-----|----------------------|-----|-------------------------------|---------|----------|------------------------|-----|------|
|           | Focals[pix]         |     | Principal point[pix] |     | Euler angles <sup>a</sup> [°] |         |          | Translation vector [m] |     |      |
|           | fx                  | fy  | u0                   | v0  | $\alpha$                      | $\beta$ | $\gamma$ | tx                     | ty  | tz   |
| 1         | 728                 | 376 | 349                  | 154 | 29                            | -35     | 195      | 2.9                    | 1.9 | -2.0 |
| 2         | 724                 | 375 | 304                  | 145 | 18                            | -59     | 194      | 4.3                    | 1.3 | -1.6 |
| 3         | 724                 | 375 | 290                  | 138 | 162                           | -53     | -15      | 4.3                    | 1.4 | 2.6  |
| 4         | 724                 | 375 | 325                  | 140 | 38                            | 29      | 159      | -1.3                   | 2.4 | -2.1 |
| 5         | 724                 | 375 | 348                  | 137 | 15                            | 70      | 165      | -3.2                   | 1.2 | -0.8 |
| 6         | 724                 | 375 | 348                  | 137 | 15                            | 70      | 165      | -3.2                   | 1.2 | -0.8 |
| 7         | 719                 | 372 | 329                  | 135 | 149                           | -27     | -16      | 2.9                    | 2.4 | 3.0  |
| 8         | 730                 | 377 | 351                  | 133 | 138                           | 26      | 20       | -1.1                   | 2.5 | 3.0  |
| 9         | 716                 | 371 | 345                  | 139 | 161                           | 69      | 16       | -3.3                   | 1.2 | 1.9  |

a. XYZ rotation sequence

TABLE II. PROPOSED METHOD: MEAN ERROR [°] BETWEEN COMPUTED AND TRUE ANGLES FOR VARIOUS AMOUNT OF ADDED GAUSS NOISE

| Cam. Num. | Gauss noise variance [pixels] |      |      |      |      |      |      |
|-----------|-------------------------------|------|------|------|------|------|------|
|           | 0                             | 0.01 | 0.02 | 0.05 | 0.2  | 0.5  | 1.0  |
| 1         | 0.0                           | 7.1  | 9.7  | 13.4 | 19.9 | 22.5 | 24.5 |
| 2         | 0.0                           | 12.1 | 15.2 | 18.8 | 23.2 | 24.7 | 26.0 |
| 3         | 0.0                           | 12.8 | 16.4 | 19.7 | 24.3 | 26.9 | 28.0 |
| 4         | 0.0                           | 4.5  | 6.1  | 8.9  | 14.0 | 17.8 | 20.1 |
| 5         | 0.0                           | 7.7  | 9.9  | 12.8 | 17.6 | 21.1 | 23.3 |
| 6         | 0.0                           | 3.7  | 5.0  | 7.4  | 11.7 | 15.4 | 17.8 |
| 7         | 0.0                           | 8.5  | 11.4 | 16.0 | 21.5 | 24.5 | 26.0 |
| 8         | 0.0                           | 5.9  | 8.0  | 11.0 | 16.9 | 20.4 | 23.2 |
| 9         | 0.0                           | 9.0  | 11.8 | 15.7 | 21.0 | 23.3 | 25.4 |

TABLE III. 'CLASSICAL' APPROACH: MEAN ERROR [°] BETWEEN COMPUTED AND TRUE ANGLES FOR VARIOUS AMOUNT OF ADDED GAUSS NOISE

| Cam.   | Gauss noise variance [pixels] |      |      |      |      |      |      |
|--------|-------------------------------|------|------|------|------|------|------|
|        | 0                             | 0.01 | 0.02 | 0.05 | 0.2  | 0.5  | 1.0  |
| CamAll | 0.0                           | 0.02 | 0.03 | 0.05 | 0.10 | 0.16 | 0.23 |
| Cam12  | 0.0                           | 0.4  | 0.6  | 0.9  | 1.8  | 2.7  | 3.9  |
| Cam13  | 0.0                           | 0.1  | 0.1  | 0.2  | 0.4  | 0.6  | 0.8  |
| Cam14  | 0.0                           | 0.1  | 0.1  | 0.2  | 0.4  | 0.7  | 1.0  |
| Cam25  | 0.0                           | 0.2  | 0.3  | 0.5  | 1.0  | 1.6  | 2.3  |
| Cam26  | 0.0                           | 0.2  | 0.3  | 0.5  | 1.0  | 1.6  | 2.3  |
| Cam27  | 0.0                           | 0.1  | 0.2  | 0.3  | 0.5  | 0.9  | 1.2  |

### IV. DISCUSSION AND CONCLUSION

The concept of computing angle between lines via its vanishing points is quite well established in computer vision literature. Yet, its real life application issues are less frequently discussed. One of the goals of this work was to test one possible implementation of mentioned concept with the aim of computing angles between human segments. Namely, during the human motion analysis it would be definitely beneficial if it were accurate method for computing angles between segments using single camera and possibly even noncalibrated one. It is quite customary to test various ideas during research first with simulated/synthetic data and afterwards perhaps proceed with real ones. That's why the proposed idea was pursued and evaluated, at least at this instance of time, solely on synthetic data. For that purpose potential structure of attached wands was

presented on Fig. 1. Then, a hypothetical spatial camera set up was chosen, with both internal and external parameters, very similar to one frequently used in practice (Table I). Based on such ideal data image coordinates were obtained of simulated angles between two wands, i.e. segments, for serious of spatial locations and angles. Afterwards, assuming Gauss noise, with zero mean, different amounts of it were added. Robustness of proposed method was evaluated by computing mean error between true angles between wands and computed one, in the environment of different amounts of noise. At the same time, angles were computed in classical way using multiple cameras. As it appears mean error obtained in case of proposed method (Table II) is quite larger then the one using 'classical' approach (Table III). Generally speaking, redundancy in processing data is beneficial. In that sense one could argue that classical approach is so much superior to proposed method simply because it uses data from multiple cameras (in our case maximum of 9). However, even in case of minimal configuration for 'classical' approach (i.e. two cameras) mean error is still considerably smaller then proposed one (Table II), although also for an order of magnitude worse then using all 9 cameras (first data row in Table III).

It is beyond the scope of this paper to carry out a comprehensive numerical analysis of computational sensitive to noise of equations involved in proposed method, particularly (6). Nevertheless some general remarks can be stated. Equation (6) consists of one factor in numerator and two factors denominator, both containing vanishing point of two lines. Therefore, potential scaling of two vanishing points would simply cancel out. Similar conclusion can be probably drawn for any transformation applied on vanishing points and image of the absolute conic in equation (6). Hence, that leaves us with conclusion that we need to improve computation of vanishing points itself.

Vanishing points are here computed from theoretical minimum of three pair correspondences and perhaps increasing the number of markers on wands might improve the accuracy. Besides, in practice, it is quite usual that wands, i.e. human segments, may appear (close to) parallel or perpendicular to the cameras image sensor. Under these circumstances presence of even a small amount of noise will cause vanishing points to be computed quite off their correct values.

A known ratio on the line is not the only way of computing vanishing points. For instance, alternative is also from two parallel lines. Therefore, potential structure (Fig. 1) could be upgraded with additional wands parallel and rigidly attached to the shown one. Of course the drawback is more complex attachment on subject's segments.

In summary, at the moment proposed method in terms of accuracy can hardly substitute 'classical' way of computing angle between segments, particularly in cases where more than

one calibrated camera is available. Furthermore, for biomechanical analysis are often of interests so-called joint angles and/or segments orientation angles which in general ask for some additional information such as segments centers of mass, joint centers ([17], [18]) etc. In despite all that, proposed method theoretically does have some clear practical advantages, mentioned earlier. Thus, in cases where only ordinary spatial angle between longitudinal axes of segments is needed, proposed method is worth of further investigations which are left for future work.

## REFERENCES

- [1] P. Allard, I. Stokes, and J-P Blachi. Three Dimensional Analysis of Human Movement. Human Kinetics, Champaign, 1995.
- [2] H.J. Woltring, and R. Huiskies. Stereophotogrammetry, Biomech. of human movement (edited by N. Beme and A. Capozzo), Bertec Corporation, Worthington, Ohio, 1990, pp. 108-127.
- [3] K.B. Atkinson. Close Range Photogrammetry and Machine Vision. Whittles Publishing, Caithness, Scotland, 1996.
- [4] J. Eian, and R.E. Poppele. A single-camera method for three-dimensional video imaging. Journal of Neuroscience Methods, 2002, 120, pp. 65-83.
- [5] R. A. Jarvis, "A perspective on range-finding techniques for computer vision, IEEE Trans. Pattern Analysis Mach. Intell., 1983, 5:122-139.
- [6] D.A. Winter. Biomechanics and motor control of human movement. John Wiley & Sons, New York, 1990.
- [7] Webster, J.G. – Editor. Camera Calibration for Image Processing. Wiley Encyclopedia of Electrical and Electronics Engineering. John Wiley, New York, 2, 743-758, 1999.
- [8] T. Pribanić, M. Cifrek and S. Tonković. Comparison of three different camera calibration types. XIVth Congress of the International Society of Electrophysiology and Kinesiology, Vienna, Austria, 2002, pp. 106-107.
- [9] Z. Zhang. A flexible new technique for camera calibration. IEEE Transactions on PAMI, 2000, 22(11):1330-1334.
- [10] N.A. Borghese and P. Cerveri. Calibrating a video camera pair with a rigid bar. Pattern Recognition, 2000, 33, pp. 81-95.
- [11] R. Hartley and A. Zisserman. Multiple View Geometry in Computer Vision, Cambridge University Press, 2000.
- [12] V.M. Zatsiorsky. Kinematics of human motion. Human Kinetics, Champaign, 1998.
- [13] V.M. Zatsiorsky. Kinetics of human motion. Human Kinetics, Champaign, 2002.
- [14] H. Baruh. Analytical Dynamics. WCB/McGraw-Hill, 1999.
- [15] J.G. Semple and G.T. Kneebone. Algebraic projective geometry. Oxford University Press, London, 1979.
- [16] T. Pribanic, P. Sturm and M. Cifrek. On the Applicability of Several Methods for Camera Calibration. 3rd European Medical and Biological Engineering Conference (EMBE'05) and IFMBE European Conference on Biomedical Engineering. November 20-25, Prag, Czech Republic. 2005, pp. 1-6.
- [17] E.S. Grood and W.J. Suntay. A joint coordinate system for the clinical description of threedimensional motions: Application to the knee. J. Biomechanical Engineering, 1983, 105, pp. 136-144.
- [18] C.L. Vaughan, B.L. Davis and J.C. O'Connor. Dynamics of Human Gait. Kiboho Publishers, Cape Town, South Africa, 1999.